

# PLY-THICKNESS EFFECT ON FIBER-MATRIX INTERFACE CRACK GROWTH

L. Di Stasio<sup>1,2</sup>, J. Varna<sup>1</sup>, Z. Ayadi<sup>2</sup>

<sup>1</sup>Division of Materials Science, Luleå University of Technology, Luleå, Sweden

<sup>2</sup>EEIGM & IJL, Université de Lorraine, Nancy, France

9<sup>th</sup> International Conference on Composite Testing and Model Identification  
Luleå (SE), May 27-29, 2019



## Outline

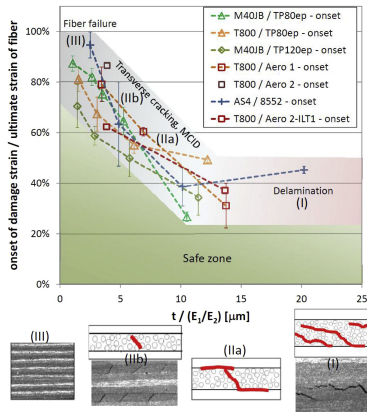
- ➔ Initiation of Transverse Cracks in Thin-plys
- ➔ Modeling the Fiber-Matrix Interface Crack
- ➔ Debond Energy Release Rate
- ➔ Conclusions



# INITIATION OF TRANSVERSE CRACKS IN THIN-PLIES

## The Thin-ply "Advantage": new material

2018,  $[45^\circ, 90^\circ, -45^\circ, 0]$  ns

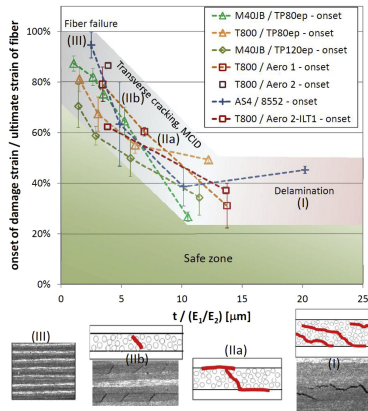


Cugnoni et al., Compos. Sci. Technol. **168**, 2018, p. 467–477.

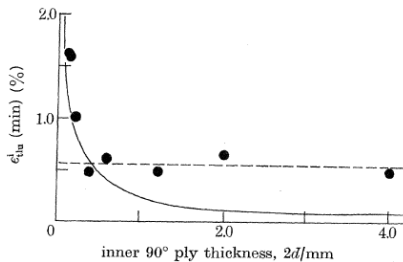
## The Thin-ply "Advantage": new material, old result

2018,  $[45^\circ, 90^\circ, -45^\circ, 0]_{ns}$

1979,  $[0^\circ, 90^\circ]_s$

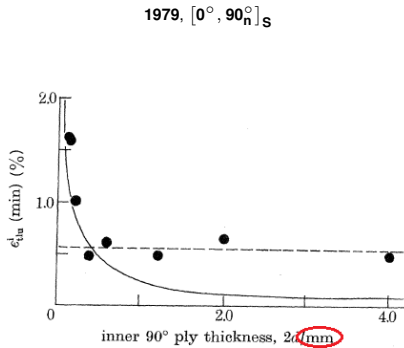
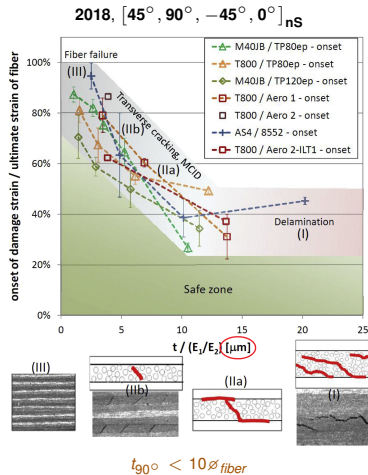


Cugnoni et al., Compos. Sci. Technol. **168**, 2018, p. 467–477.



Bailey et al., P. Roy. Soc. A-Math. Phys. **366** (1727), 1979.

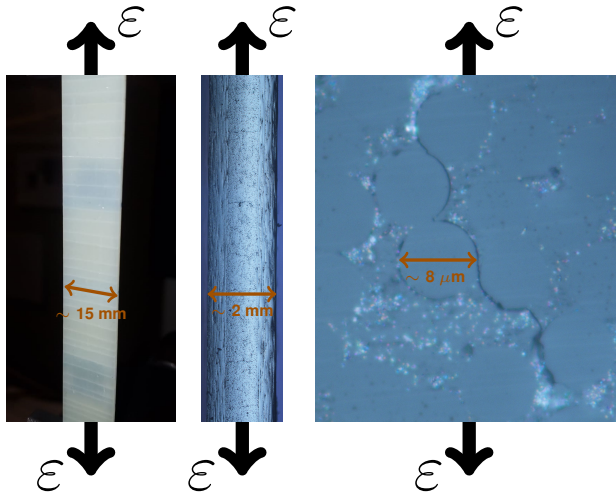
## The Thin-ply "Advantage": new material, old result?



Cugnoni et al., Compos. Sci. Technol. **168**, 2018.

Bailey et al., P. Roy. Soc. A-Math. Phys. **366** (1727), 1979.

## Micromechanics of Initiation



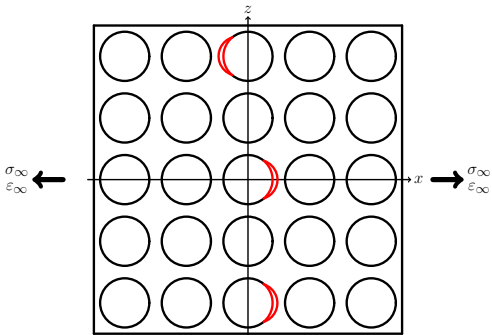
**Left:**  
front view of  $[0, 90]_S$ ,  
visual inspection.

**Center:**  
edge view of  $[0, 90]_S$ ,  
optical microscope.

**Right:**  
edge view of  $[0, 90]_S$ ,  
optical microscope.

## Micromechanics of Initiation

### Stage 1: isolated debonds



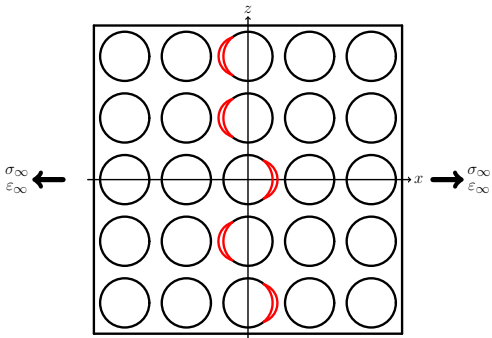
Bailey et al., P. Roy. Soc. A-Math. Phy. **366** (1727), 1979.

Bailey et al., J. Mater. Sci. **16** (3), 1981.

Zhang et al., Compos. Part A-Appl. S. **28** (4), 1997.

## Micromechanics of Initiation

### Stage 2: consecutive debonds



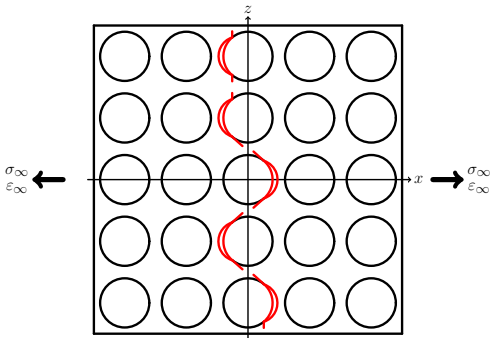
Bailey et al., P. Roy. Soc. A-Math. Phy. **366** (1727), 1979.

Bailey et al., J. Mater. Sci. **16** (3), 1981.

Zhang et al., Compos. Part A-Appl. S. **28** (4), 1997.

## Micromechanics of Initiation

### Stage 3: kinking



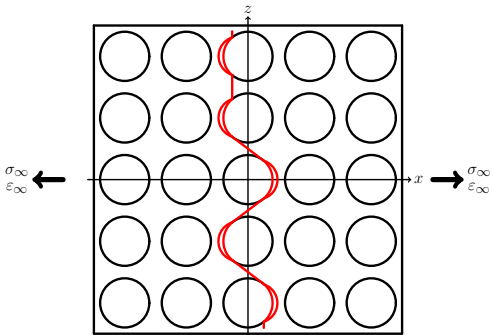
Bailey et al., P. Roy. Soc. A-Math. Phy. **366** (1727), 1979.

Bailey et al., J. Mater. Sci. **16** (3), 1981.

Zhang et al., Compos. Part A-Appl. S. **28** (4), 1997.

## Micromechanics of Initiation

### Stage 4: coalescence



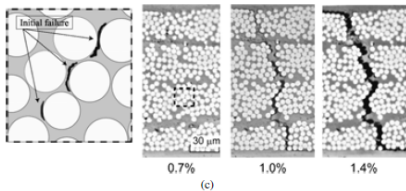
Bailey et al., P. Roy. Soc. A-Math. Phy. **366** (1727), 1979.

Bailey et al., J. Mater. Sci. **16** (3), 1981.

Zhang et al., Compos. Part A-Appl. S. **28** (4), 1997.

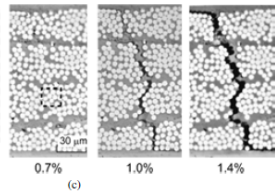
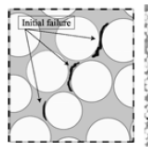
## A Counter-intuitive Observation

$[0^\circ, 90_n^\circ]_S$

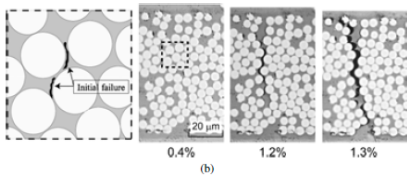


## A Counter-intuitive Observation

$[0^\circ, 90_n^\circ]_S$



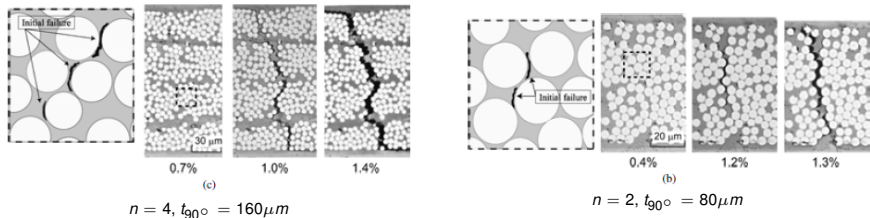
$$n = 4, t_{90^\circ} = 160 \mu m$$



$$n = 2, t_{90^\circ} = 80 \mu m$$

## A Counter-intuitive Observation

$[0^\circ, 90^\circ]_S$

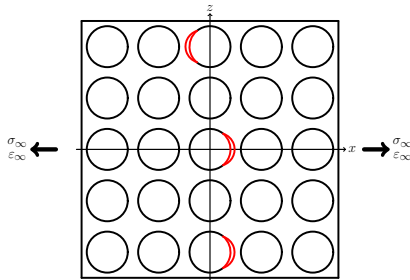


Saito et al., Adv. Compos. Mater. 21 (1), 2012.

## Objective of the Study

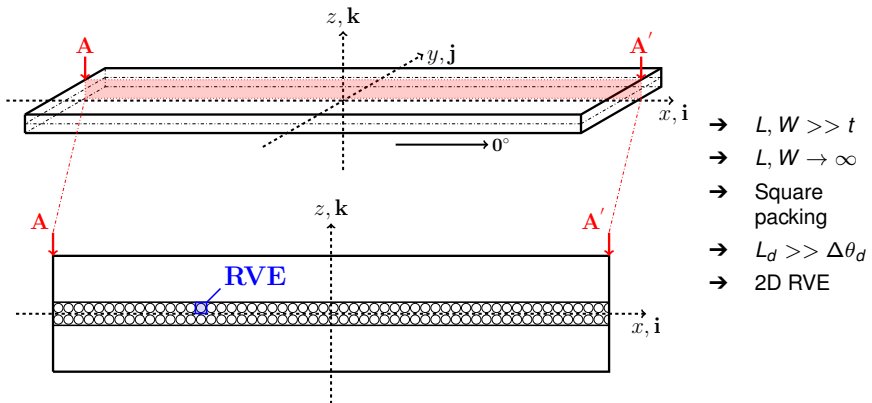
Can we talk about a ply-thickness effect for the fiber-matrix interface crack?

### Stage 1: isolated debonds

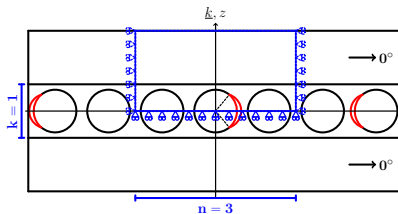


# **MODELING THE FIBER-MATRIX INTERFACE CRACK**

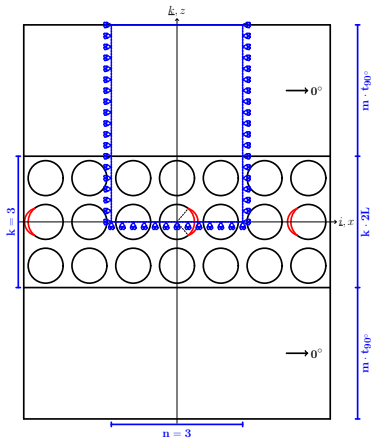
## Geometry



## Representative Volume Elements

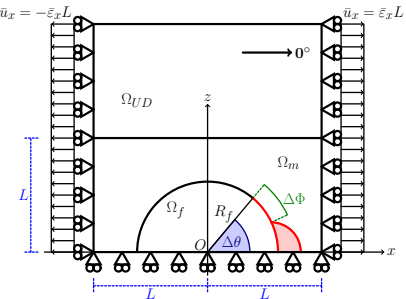


$$n \times 1 - m \cdot t_{90^\circ}$$



$$n \times k - m \cdot t_{90^\circ}$$

## Assumptions

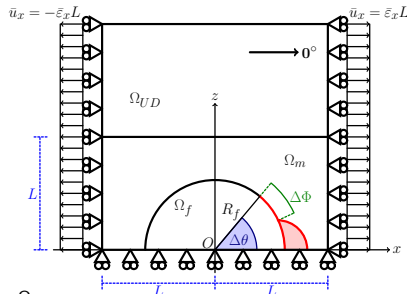


$$R_f = 1 \text{ } [\mu\text{m}] \quad L = \frac{R_f}{2} \sqrt{\frac{\pi}{V_f}}$$

- Linear elastic, homogeneous materials
- Concentric Cylinders Assembly with Self-Consistent Shear Model for UD
- Plane strain
- Frictionless contact interaction
- Symmetric w.r.t. x-axis
- Coupling of x-displacements on left and right side (repeating unit cell)
- Applied uniaxial tensile strain  $\bar{\varepsilon}_x = 1\%$
- $V_f = 60\%$

Material	$V_f$ [%]	$E_L$ [GPa]	$E_T$ [GPa]	$\mu_{LT}$ [GPa]	$\nu_{LT}$ [-]	$\nu_{TT}$ [-]
Glass fiber	-	70.0	70.0	29.2	0.2	0.2
Epoxy	-	3.5	3.5	1.25	0.4	0.4
UD	60.0	43.442	13.714	4.315	0.273	0.465

## Solution



in  $\Omega_f$ ,  $\Omega_m$ ,  $\Omega_{UD}$ :

$$\frac{\partial^2 \varepsilon_{xx}}{\partial z^2} + \frac{\partial^2 \varepsilon_{zz}}{\partial x^2} = \frac{\partial^2 \gamma_{zx}}{\partial x \partial z} \quad \text{for } 0^\circ \leq \alpha \leq \Delta\theta : \quad (\vec{U}_m(R_f, \alpha) - \vec{U}_f(R_f, \alpha)) \cdot \vec{n}_\alpha \geq 0$$

$$\varepsilon_y = \gamma_{xy} = \gamma_{yz} = 0$$

$$\frac{\partial \sigma_{xx}}{\partial x} + \frac{\partial \tau_{zx}}{\partial z} = 0 \quad \text{for } \Delta\theta \leq \alpha \leq 180^\circ : \quad \vec{U}_m(R_f, \alpha) - \vec{U}_f(R_f, \alpha) = 0$$

$$\frac{\partial \tau_{zx}}{\partial x} + \frac{\partial \sigma_{zz}}{\partial z} = 0 \quad \sigma_{ij} = E_{ijkl} \varepsilon_{kl}$$

$$\sigma_{yy} = \nu (\sigma_{xx} + \sigma_{zz})$$

→ Oscillating singularity

$$\sigma \sim r^{-\frac{1}{2}} \sin(\varepsilon \log r), \quad V_f \rightarrow 0$$

$$\varepsilon = \frac{1}{2\pi} \log \left( \frac{1-\beta}{1+\beta} \right)$$

$$\beta = \frac{\mu_2(\kappa_1 - 1) - \mu_1(\kappa_2 - 1)}{\mu_2(\kappa_1 + 1) + \mu_1(\kappa_2 + 1)}$$

$$\rightarrow G = \frac{\partial W}{\partial A} - \left( \frac{\partial U}{\partial A} + \frac{\partial E_k}{\partial A} \right)$$

→ Finite Element Method (FEM)  
in Abaqus™

→ 2<sup>nd</sup> order shape functions

→ 6-nodes triangles & 8-nodes quadrilaterals

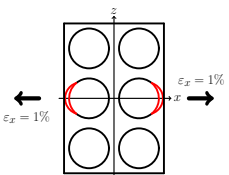
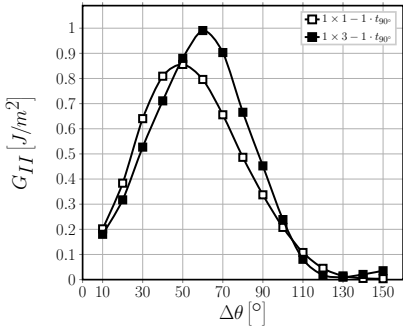
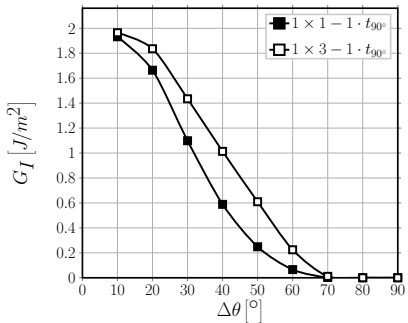
→ regular mesh of quadrilaterals  
at the crack tip:

- $AR \sim 1$
- $\delta = 0.05^\circ$

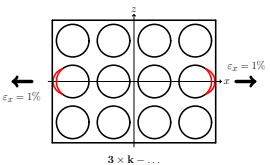
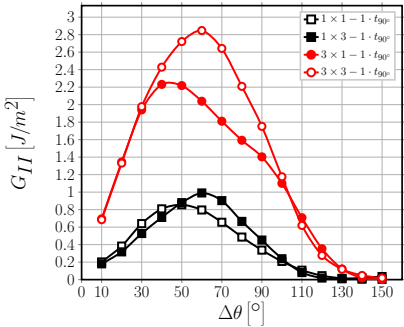
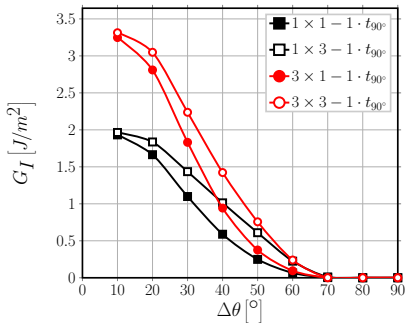
Initiation of Transverse Cracks in Thin-plies   Modeling the Fiber-Matrix Interface Crack   Debond Energy Release Rate   Conclusions  
Interaction of Debonds   Effect of 0° ply thickness   Effect of 90° ply thickness

## DEBOND ENERGY RELEASE RATE

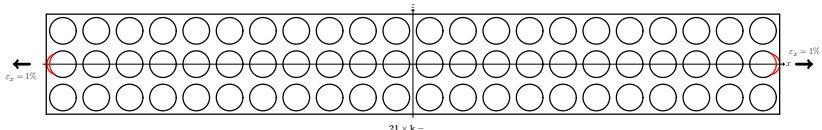
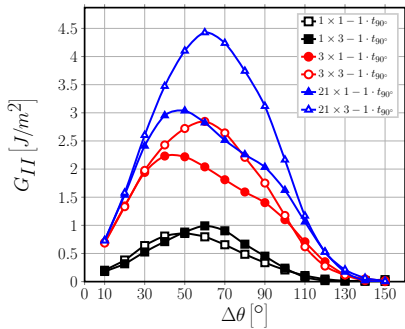
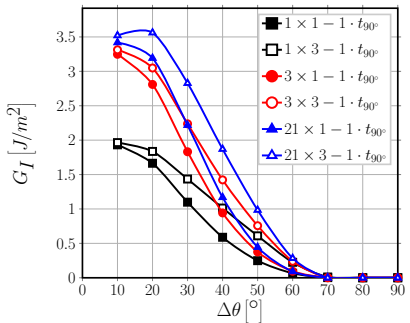
## Interaction of Debonds: Strain Magnification



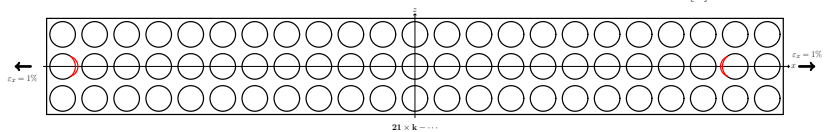
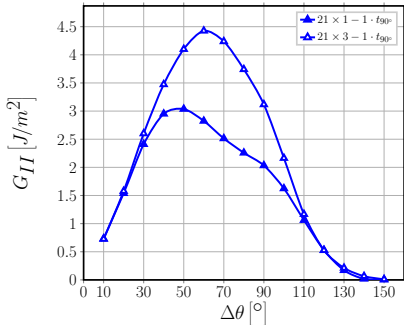
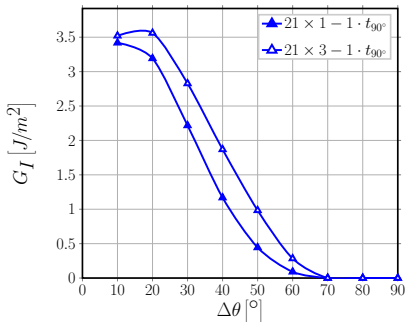
## Interaction of Debonds: Strain Magnification



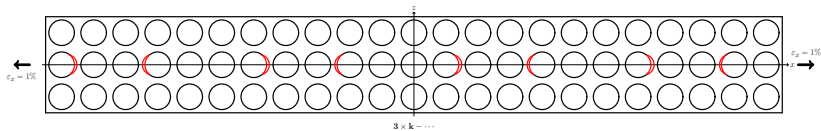
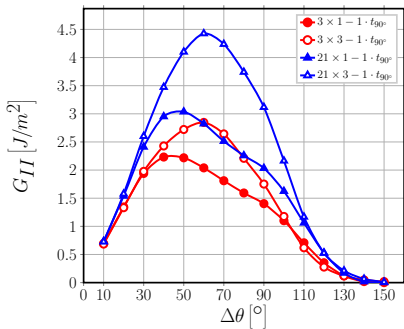
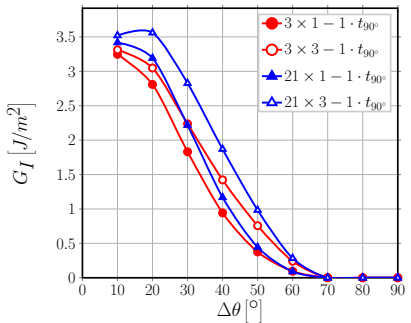
## Interaction of Debonds: Strain Magnification



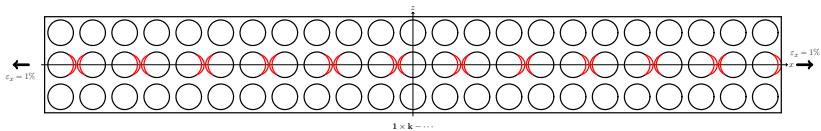
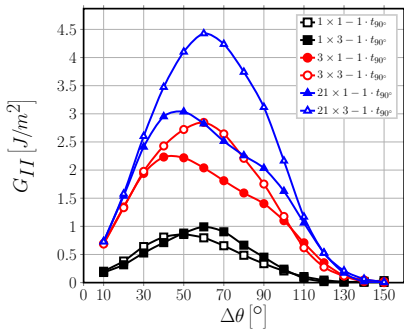
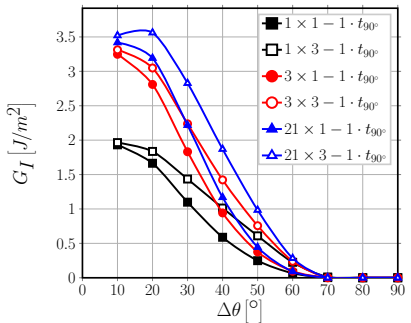
## Interaction of Debonds: Crack Shielding



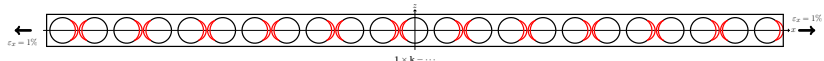
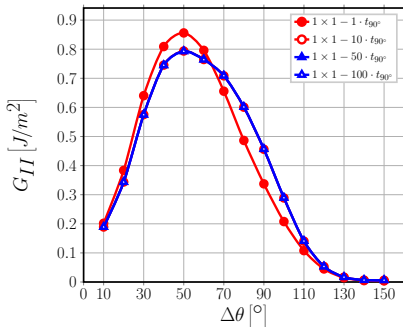
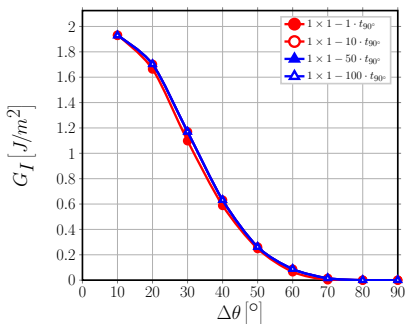
## Interaction of Debonds: Crack Shielding



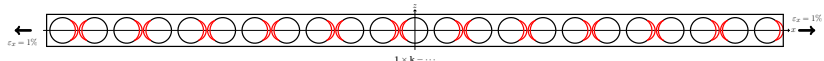
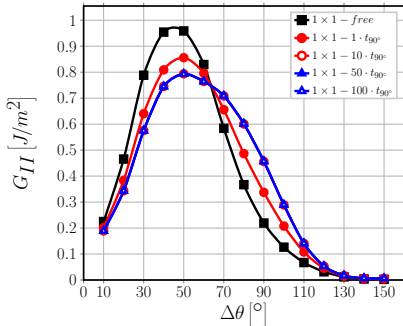
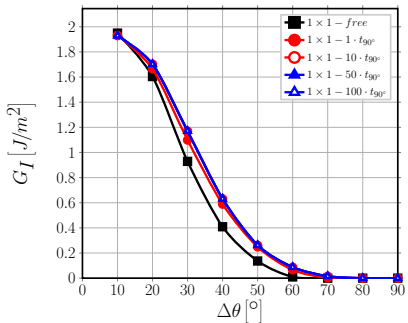
## Interaction of Debonds: Crack Shielding



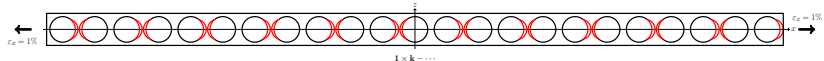
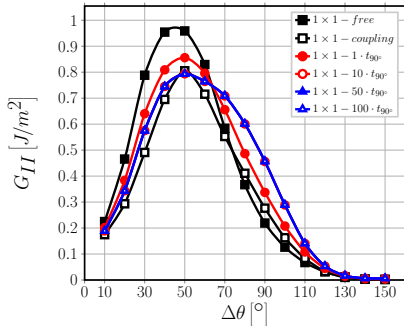
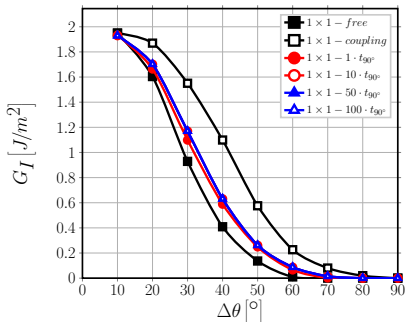
## Effect of 0° ply thickness



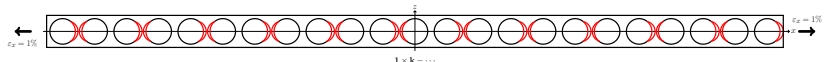
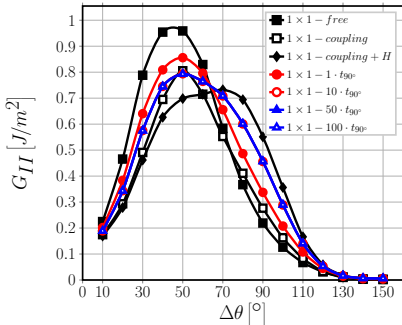
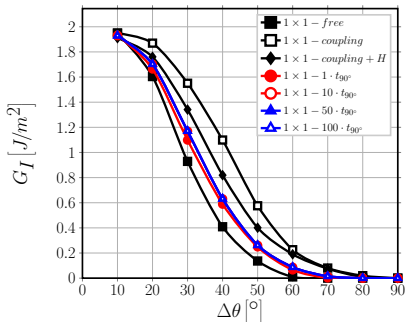
## Effect of $0^\circ$ ply thickness



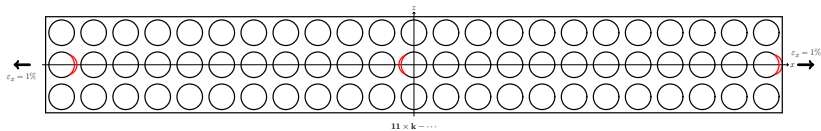
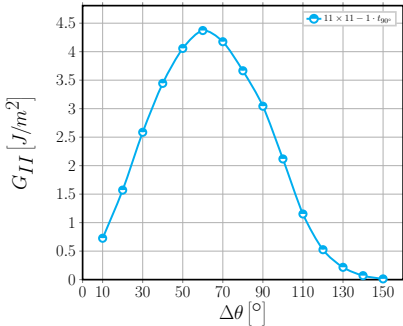
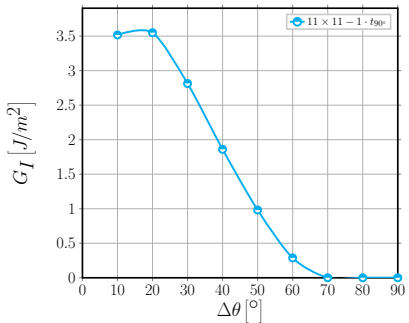
## Effect of 0° ply thickness



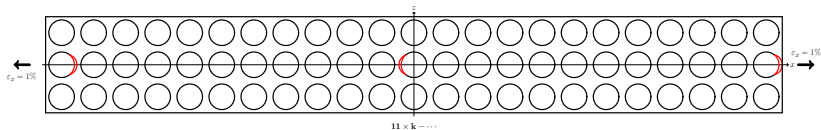
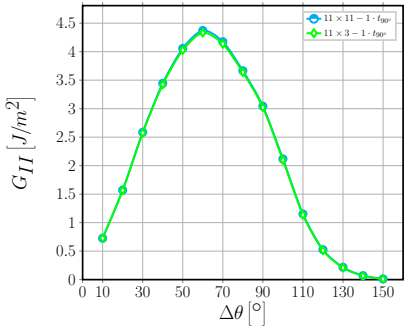
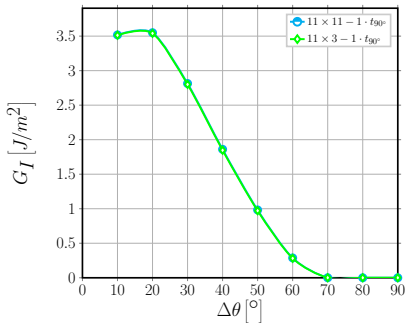
## Effect of 0° ply thickness



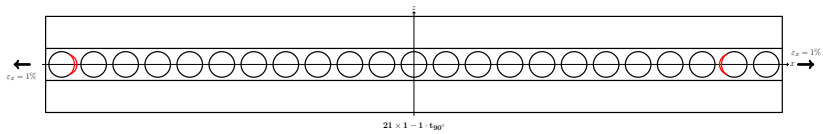
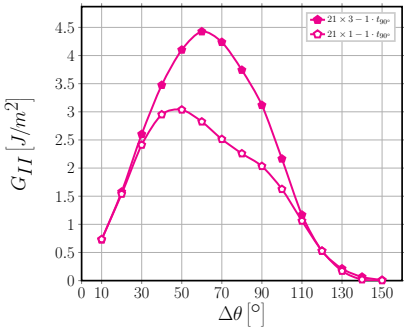
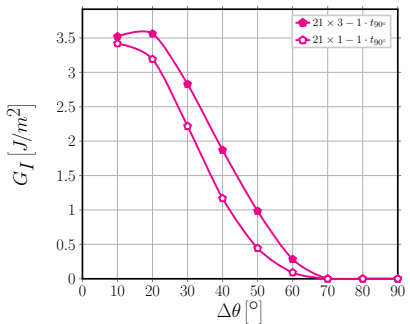
## Effect of 90° ply thickness



## Effect of 90° ply thickness



## Effect of 90° ply thickness



## CONCLUSIONS

## Conclusions

- Debond-debond interaction in the through-the-thickness direction is extremely localized: with only a couple of undamaged fibers in between, no effect can be seen!
- For debonds on consecutive vertically-aligned fibers,  $G_{II}$  is higher and contact zone onset delayed if debonds are on the same side of their respective fiber.
- No significant difference in  $G_{II}$  observed, except in the range  $80^\circ - 100^\circ$ .
- In the range  $80^\circ - 100^\circ$ ,  $G_{II}$  is higher when debonds are located on opposite sides of consecutive vertically-aligned fibers.



LULEÅ  
UNIVERSITY  
OF TECHNOLOGY



Education and Culture

Erasmus Mundus